

1 **Improving power quality efficient in demand response: aggregated heating, ventilation and**  
2 **air-conditioning systems**

3  
4  
5 Authorship

6  
7 **Xu-Dong Chen**

8 1. State Key Laboratory of Reliability and Intelligence of Electrical Equipment, Hebei  
9 University of Technology, Tianjin 300130, China;

10 2. School of Electronic Information Engineering, Rizhao Polytechnic, Shandong 276826,  
11 China

12 E-mail: [bensonxchen@126.com](mailto:bensonxchen@126.com)

13  
14 **Lingling Li**

15 1. State Key Laboratory of Reliability and Intelligence of Electrical Equipment, Hebei  
16 University of Technology, Tianjin 300130, China;

17 2. Key Laboratory of Electromagnetic Field and Electrical Apparatus Reliability of Hebei  
18 Province, Hebei University of Technology, Tianjin 300130, China

19 E-mail: [lilinglinglaoshi@126.com](mailto:lilinglinglaoshi@126.com); [lilingling@hebut.edu.cn](mailto:lilingling@hebut.edu.cn)

20  
21 **Ming-Lang Tseng \***

22 1. Institute of Innovation and Circular Economy, Asia University, Taiwan;

23 2. Department of Medical Research, China Medical University Hospital, Taiwan

24 3. Faculty of Economics and Management, Universiti Kebangsaan Malaysia, Malaysia

25 E-Mail : [tsengminglang@gmail.com](mailto:tsengminglang@gmail.com); [Tsengminglang@asia.edu.tw](mailto:Tsengminglang@asia.edu.tw)

26  
27 **Kimhua Tan**

28 School of Business, University of Nottingham, United Kingdom

29 E-mail: [kim.tan@nottingham.ac.uk](mailto:kim.tan@nottingham.ac.uk)

30  
31 **Mohd Helmi Ali**

32 National University of Malaysia Faculty of Economic and Management, Malaysia

33 E-mail: [mohdhelmiali@ukm.edu.my](mailto:mohdhelmiali@ukm.edu.my)

47 **Improving power quality efficient in demand response: aggregated heating, ventilation and**  
48 **air-conditioning systems**

49  
50

51 **ABSTRACT**

52 This study aims to identify the role of aggregated heating, ventilation, and air  
53 conditioning (HVAC) loads based on system characteristics using the lazy state switching  
54 control mode focusing on the overall power consumption rather individual response speed.  
55 This study is attempted to provide secondary frequency regulation using aggregated HVAC  
56 loads with more stable operation with the lazy state switching control mode based on  
57 conditional switching of the HVAC unit's working state. The stability of power consumption  
58 improves power quality in smart grid design and operation. The aggregated HVAC must reach  
59 a stable condition before tracking the automatic generation control signal and fully  
60 developed smart grids complex structure. Still, HVAC slowed responses make inappropriate  
61 for faster demand response services. Unsuitable control algorithm leads to system instability  
62 and HVAC unit overuse. An extended command processing on the client side is proposed to  
63 deal with the adjusting command. The unique advantages of the proposed algorithm are  
64 three folds. (1) the control algorithm preserves its working state and has nothing conflicting  
65 with the lockout constraints for individual system units; (2) the control algorithm shows  
66 promising performance in smoothing the overall power consumption for the aggregated  
67 population; and (3) the control logic is fully compatible with other control algorithms. The  
68 proposed modeling and control strategy are validated against simulations of thousands of  
69 units, and the simulation result indicates that the proposed approach has promising  
70 performance in smoothing the power consumption of aggregate units' population.

71

72 **Keywords:** Renewable energy; Smart Grid; Demand response; Power quality; Heating,  
73 ventilation and air conditioning (HVAC); Lazy state switching.

74

75

76

77

78

79

80

81

82

83

84

85

86

87

88

89

90

91

92

93

94 **Improving power quality efficient in demand response: aggregated heating, ventilation and**  
 95 **air-conditioning systems**

Nomenclature	
Abbreviations	
AGC	automatic generation control
DR	demand response
ETP	equivalent thermal parameter
HEMS	home energy management system
HVAC	Heating, ventilation, and air conditioning
LSS	lazy state switching
TCL	thermostatically controlled loads
PEV	plug-in electric vehicles
Indices	
$i$	index of state-space
$t$	index of time
Variables and parameters	
$x_a$	inner air temperature (°F) of HVAC unit
$x_m$	inner mass temperature (°F) of HVAC unit
$T_o$	outside air temperature (°F)
$U_a$	thermal conductance (Btu/hr.°F) of the building envelope
$H_m$	thermal conductance (Btu/hr.°F) between the inner air and inner solid mass
$Q_a$	the heat flux (Btu/hr) into the inner air mass
$Q_m$	heat flux (Btu/hr) to the inner solid mass
$C_a$	thermal mass (Btu/°F) of the internal air
$C_m$	thermal mass (Btu/°F) of the building materials and furniture
$U_{set}$	HVAC temperature (°F) setpoint
$\delta$	HVAC unit's temperature (°F) deadband
$T_{a,min}$	minimal air temperature (°F) for a population of HVAC loads
$T_{a,max}$	maximum air temperature (°F) for a population of HVAC loads
$T_{sp,i}$	temperature setpoint (°F) of HVAC unit $i$
$\Delta T_{sp}$	the amount of temperature setpoint change
$S$	the working state of an HVAC unit
$\epsilon_t$	an infinitesimal time delay
$f_i^*$	the probability for an HVAC unit to reside in a certain temperature segment
$\Delta m_i^{on/off}$	the number of HVAC units in state $i$ at a given moment
$n$	the total number of HVAC units in the simulation tests
$P$	power consumption (W) of single HVAC unit
$P_{HVAC}$	total power consumption (W) of the aggregated loads
$\eta$	power system's transmission efficiency
$\Delta P$	instantaneous power increase
$U_c(\mu_*, \delta_*)$	represents a uniform distribution centered by $\mu_*$ , and spans the distance $\delta_*$
$\delta_m$	parameters deadband vector
Uniform(*,*)	Uniform distribution between two values
Uc(*,*)	uniform distribution center by the first value with deadband of the second value
$\mu_{Af}$	center value of floor area (ft <sup>2</sup> )
$\mu_{Ia}$	center value of air exchange (1/hr)
$\mu_{Rc}$	center value of roof R-value (°F.ft <sup>2</sup> .hr/Btu)
$\mu_{Rw}$	center value of wall R-value (°F.ft <sup>2</sup> .hr/Btu)
$\mu_{Rf}$	center value of floor R-value (°F.ft <sup>2</sup> .hr/Btu)
$\mu_{Rd}$	center value of door R-value (°F.ft <sup>2</sup> .hr/Btu)
$\delta_{Af}$	deadband of floor area distribution
$\delta_{Ia}$	deadband of air exchange distribution
$\delta_{Rc}$	deadband of roof R-Value distribution
$\delta_{Rw}$	deadband of wall R-Value distribution
$\delta_{Rf}$	deadband of floor R-Value distribution
$\delta_{Rd}$	deadband of door R-Value distribution
$R_{on}$	ratio of "on" units in aggregated HVAC loads

96

97

98

99

100

101 **Improving power quality efficient in demand response: aggregated heating, ventilation and**  
102 **air-conditioning systems**  
103

104 **1. Introduction**

105 Future smart grid, power quality has gained particular importance due to increase number  
106 of sensitive loads and faces new challenges (Bidram and Davoudi 2012). Especially, variable  
107 renewable energy generation and unstable load demand are both sources of uncertainties in  
108 the grid (Eksin et al. 2015). At the supply side, renewables, such as solar and wind energy,  
109 are established as mainstream sources of energy (Ismail et al. 2019). Renewables have  
110 undergone rapid growth globally and supply 40% of the world's energy. They are expected  
111 to play a major role in the future power generation by 2040 (Cai and Braun 2019; Sedady  
112 and Beheshtinia, 2019). However, the integration of large-scale renewable energy affects the  
113 power system in many ways. The intermittent nature of renewable energy presents  
114 significant challenges on system security and operation, when a larger proportion of  
115 renewable energy sources are integrated in, e.g., more than 20% (Pourmousavi et al., 2014;  
116 Zhu et al., 2015). If the penetration of renewables is around 50% or more, the traditional  
117 automatic generation control (AGC) is incapable to maintain the frequency within acceptable  
118 limits (Malik and Ravishankar 2018). The power grid needs new resources for frequency  
119 reserves to provide high quality power supply.

120 As a cost-effective balancing resource, demand response (DR) is supposed to provide  
121 balancing service, which used to be provided by conventional generation units (Jin et al.,  
122 2018; Müller and Jansen 2019). Prior studies presented various types of candidate loads for  
123 DR, including thermostatically controlled loads (TCL) and plug-in electric vehicles (Antti et al.,  
124 2019; Hamidreza et al., 2019). Among these, heating, ventilation, and air conditioning  
125 (HVAC) account for 50% of total building energy consumption (Ma et al. 2019). The HVAC  
126 systems are becoming more and more popular, driven by economic growth and the desire  
127 for a better life. It is estimated that power consumption of HVAC systems will increase 33  
128 times by the end of this century (Ma et al., 2019). The systems have larger heat capacity and  
129 longer cyclic time, and they are more susceptible to outer climatic conditions (Giwa et al.,  
130 2019; Vakiloroyaya, 2014). The heat capacity of buildings act as a battery; the energy  
131 increases when the HVAC unit is on (charging) and decreases when the unit is off  
132 (discharging). The elasticity of HVAC power consumption is utilized to reduce the user's  
133 energy cost and provides DR services such as peak shaving and ancillary services (Ji et al.,  
134 2014; Lu, 2012; Nguyen and Le, 2014). The HVAC systems potential for DR needs to be  
135 evaluated.

136 Several methods for modeling and control of aggregated HVAC systems have been  
137 proposed, including direct load control and indirect load control. For instance, Wang et al.  
138 (2014) developed highly accurate modeling and control strategies based on the control  
139 center for large population of HVAC loads, wherein the HVAC loads execute commands from  
140 the control center unconditionally. These control modes act quickly, but some limitations  
141 exist: (1) The lockout constraint has little effect on normal operations but drastically affects  
142 the collective response for a large number of HVAC aggregated together because it needs to  
143 interrupt their normal operations frequently; (2) Most control algorithms have to choose  
144 between computing accuracy and system performance. The models with first-order  
145 equivalent thermal parameter (ETP) model show better performance but larger computing  
146 error. Models based on the second-order ETP have been extensively studied nowadays; they

147 show relatively high computing accuracy but put a heavy calculation burden on the control  
148 center with lower performance (Bashash and Fathy, 2013; Zhang et al., 2013); (3) The  
149 control algorithms may face serious power flickers and fluctuations due to synchronized  
150 state switching of multiple HVAC units when adjusting their thermostat setpoints, with the  
151 peak power when all units are “on” and the minimum power when all units are “off”. To  
152 suppress the power variation, the algorithm becomes more complex. (4) The control  
153 algorithms increase the frequency of unit’s on/off switching.

154 Zheng and Cai (2014) found that the number of on/off cycles was about 0–3 cycles per  
155 hour without DR control and increased to about 1–20 cycles per hour using various DR  
156 control algorithms. These issues considerably increased the operation cost of DR control  
157 algorithms. Li et al. (2017) proposed the lazy state switching (LSS) control concept for  
158 aggregated HVAC loads. This study aims to improve the control algorithm and provide  
159 secondary frequency regulation services in a fully developed smart grid environment by  
160 controlling a large number of HVAC loads. The main contributions are summarized as  
161 follows.

- 162 1. This study ensures safe and stable operations of users’ HVAC systems, to protect users’  
163 load, and to preserve system stability, reducing the frequency of unit’s on/off switching.  
164 This works well with the lockout effect and to minimize users’ electricity bills as well as to  
165 smoothen the total demand curve, and make the DR control more acceptable to users.
- 166 2. This study proposes the idea of homogeneity control to realize controlling the  
167 parameters’ distribution interval. One can test the aggregated system performance of  
168 different homogeneities to verify the adaptability of the control methods.
- 169 3. The proposed control algorithm is fully compatible with other control algorithms, and  
170 integrates into the same DR systems with other control algorithms, which enables a DR  
171 system to have multiple control modes at the same time.
- 172 4. The proposed modeling and control method is validated using GridLAB-D, which is  
173 capable of simultaneously simulating thousands of unique buildings using the second  
174 order ETP model (GridLAB-D 2012). Simulation results show that the proposed control  
175 algorithm effectively eliminate power flicker and power fluctuation and quickly restore  
176 the system to a steady state after the control center broadcasts commands to adjust the  
177 HVAC setpoint.

178 The rest of this study is organized as follows. Section 2 briefly reviews related literatures.  
179 Section 3 discusses the characteristics of HVAC units. Section 4 develops the temperature  
180 distribution model for aggregated populations of HVAC units. The improved LSS control  
181 mode is developed in Section 5. The experiment results and discussions are explained in  
182 Section 6. Finally, conclusions and future studies are presented in Section 7.

183

## 184 **2. Literature Review**

185 The structure of a smart grid is highly complicated with high penetration of renewable  
186 generation, contains lots of nonlinear or sensitive loads, and requires power supply with  
187 higher quality and stability (Pourmousavi et al., 2014; Sedady and Beheshtinia, 2019).  
188 Although numerous studies have focused on aggregate HVAC to smoothen the fluctuations  
189 of renewable generation, the power quality problems caused by the DR system itself have  
190 been overlooked. The system voltage and frequency seriously affected by the variation in  
191 load demand (Kabache et al. 2014). The switching of high-power loads imposes a  
192 considerable impact on the power grid and produces the same effect when switching large  
193 amount of loads at the same time (Zhang et al., 2013). Power fluctuations may cause various

194 problems, including voltage flicker and frequency deviation, incurring poor power supply for  
195 consumers, which causes lights to flicker and may damage useful electronic equipment  
196 (Abdul et al., 2014). This is a potential problem in aggregated DR systems, especially in HVAC  
197 load-based systems.

198 Prior studies have focused on DR systems to provide ancillary service, which is an  
199 important electric service, and the system is used by residential, commercial, or industrial  
200 users (Cui and Zhou 2018; Ma et al. 2017). The system realizes the communication between  
201 grid utilities and customers, guides users to schedule power consumption to save energy,  
202 reduces costs, and helps grid operation (Muhammad et al., 2019; Ma et al., 2017). As a  
203 representative TCL, HVAC units are studied extensively in the literature. Some studies have  
204 regulated HVAC units by turning them on or off directly at the customer premises. Lu et al.  
205 (2005) presented a state-queuing model and a temperature priority list strategy to control  
206 on/off states of HVAC units. Vanouni and Lu (2015) presented a centralized control method  
207 to provide continuous regulation services. Zhou et al. (2017) proposed a novel two-level  
208 scheduling method to minimize the power imbalance cost. Hao et al. (2015) modeled the  
209 aggregated HVAC as a stochastic energy storage battery and proposed a priority-stack-based  
210 control to control the power consumption to follow AGC signals and reduce the tracking  
211 errors by the on/off states directly. However, direct HVAC regulation does not consider the  
212 temperature setpoint and the deadband, and the tracking error is very large when large  
213 number of loads toggle their working state simultaneously (Ma et al. 2017).

214 Adjusting the HVAC setpoint is a control method for the regulation of HVAC units (Yin et  
215 al., 2016). It is the key to study the load temperature dynamics for aggregated systems of  
216 thousands of HVAC units (Adhikari et al., 2018). Lu and Chassin (2004) proposed a  
217 state-queuing mode of setpoint adjusting based on price response and analyzed the  
218 degeneracy of states followed by a damping process. The control center or the operator  
219 needs to adjust the system on a timely basis, so it is hard for the system to reach a stable  
220 state. It was concluded that the aggregated system cannot respond to AGC signals before  
221 achieving a stable condition (Bashash and Fathy, 2013). To improve stability, Bashash and  
222 Fathy (2013) developed Lyapunov-stable sliding mode controller based on a Monte Carlo  
223 model for real-time management of thermostatic air conditioning loads, assuming that  
224 communication is accessible and loads quickly respond, without considering the  
225 synchronized operation of multiple loads and their impacts on the power system. However,  
226 sliding mode control is well known for its chattering effect.

227 Zhang et al. (2013) analyzed the inner air and mass temperature and proposed a 2D  
228 temperature evolution model. They then developed a highly accurate aggregated model. At  
229 the same time, the increased communication data require high-speed communication  
230 equipment and quick response HVAC units. Tindemans et al. (2015) developed a heuristic  
231 algorithm based on setpoint adjusting for decentralized implementation. Setpoint  
232 adjustment enlarges the energy storage capacity, but it often causes large chattering effects  
233 and tracking errors (Ma et al., 2017; Gowa et al., 2019). The reason is that all HVAC units  
234 change their setpoint instantaneously when they receive control signals, resulting in many  
235 loads changing their working state simultaneously.

236 Communication latency is another important part of the total response time. In future  
237 smart grids, each HVAC unit may be under the control of a different home energy  
238 management system (HEMS). The DR client does not communicate with the DR server  
239 directly, and the HEMS communicates with the DR server on behalf of the HVAC unit (Yan et  
240 al., 2017). The network traffic and transmission speed are limited. From the perspective of

241 load characteristics, a typical residential HVAC system switches 0–3 times per hour without  
 242 DR control (Zheng and Cai 2014). Its long working cycle, slow response, and potentially  
 243 higher frequency on/off cycling make them inappropriate for fast DR service (Beil et al.,  
 244 2016).

245 Achieving users' engagement for DR system is required from the viewpoint of system  
 246 implementation (Parrish et al. 2019). The utility and system operator may expect customers  
 247 to implement home automation, enroll in some DR systems, and respond predictably to DR  
 248 signals (Ghanem and Mander 2014). However, consumer participation in DR may not follow  
 249 these expectations. It is supposed that DR participation is voluntary rather than compulsory  
 250 through regulation (Parrish et al., 2019). The potential uncertainties and risks require  
 251 decision-making whether to engage or not to conduct a cost-benefit analysis to be  
 252 considered (Jordehi, 2019). The cost of DR includes the initial investment involving the  
 253 technology's cost and preparation of a response schedule. Possible risks include discomfort  
 254 cost, rescheduling and on-site generation cost, and unexpected operations imposed on a  
 255 load. At present, the DR penetration level is small; for example, it is only 6% in the U.S. (Wei  
 256 et al., 2016). The users benefit more systematically when a DR system is designed to improve  
 257 user engagement. It is important to protect their load from overuse in addition to the limited  
 258 reduction in consumer bills. The risk of unexpected operations to the load is likely to  
 259 dissuade many customers from DR participation.

260 In summary, advanced DR system designs maintain power quality and grid stability  
 261 while properly taking advantage of the HVAC units' operation characteristics, completely  
 262 considering the users' interests and the risks imposed on the loads. This study aims to  
 263 provide secondary frequency control with a large number of HVAC units, which has fewer  
 264 requirements on communication network, has higher stability of whole power consumption,  
 265 and tends to protect user loads at the same time.

### 266 3. HVAC Unit Dynamic Model

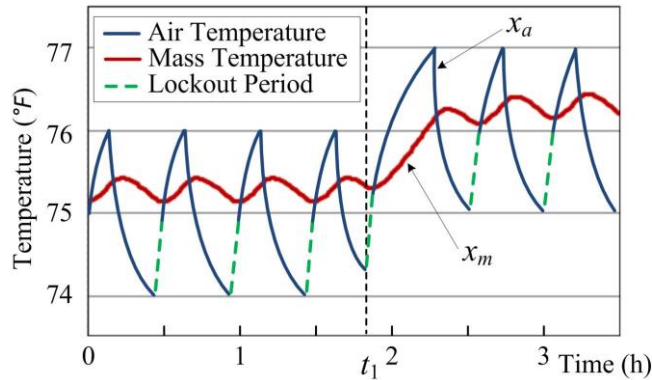
267 The characteristics of a single HVAC unit form the basis to develop an aggregated load  
 268 control model. Containing numerous variables and constraints, an HVAC system is a  
 269 complex, nonlinear, and discrete system (Khasawneh 2014). HVAC systems have a large heat  
 270 capacity and long cyclic time, and they are more susceptible to outer climatic conditions  
 271 (Vakiloroaya 2014). The dynamics of inner air temperature is studied based on the second  
 272 order ETP model (GridLAB-D 2012). The compressor time delay constraint is also discussed,  
 273 which is important in aggregated load control modeling.

274 Residential HVAC units belong to different users and are controlled individually by  
 275 simple hysteresis controllers. Prior studies described the thermodynamics of an HVAC unit  
 276 (Zhang et al., 2013). This study adopted the popular ETP model to describe the dynamics of  
 277 air and mass temperature using two coupled first-ordered ODE (GridLAB-D 2012).

$$279 \begin{cases} \frac{dx_a}{dt} = \frac{1}{C_a} [-(U_a + H_m)x_a + H_m x_M + U_a T_o + Q_a] \\ \frac{dx_m}{dt} = \frac{1}{C_m} [H_m x_a - H_m x_m + Q_m] \end{cases} \quad (1)$$

280 For a given HVAC system with known initial conditions, the solution trajectory for  $x_a$  is  
 281 uniquely determined. Figure 1 shows typical coupled air and mass temperature trajectories  
 282 with setpoint  $U_{set} = 75^\circ\text{F}$ , deadband  $\delta = 2^\circ\text{F}$ , and initial outside air temperature  
 283  $T_o = 90^\circ\text{F}$ .  $t_1$  indicates the time when the unit's setpoint is raised by 1 °F. The air  
 284

285 temperature trajectory is different for each working cycle, especially when the thermostat  
 286 setpoint is changed. The green dashed lines indicate the time period when the unit remains  
 287 off, ignoring the switching on signals due to the lockout effect.  
 288



289  
 290 Figure 1 Characteristics of a single HVAC unit  
 291

292 The lockout effect is an important protection function to ensure the compressor remains  
 293 off for certain amount of time, e.g. 5 min. During this period, the high pressure in the  
 294 compressor chamber is released. It may cause physical damage if the compressor restarts  
 295 early under pressure (Zhang et al., 2013). The lockout effect does not affect normal  
 296 operations. However, it can seriously impact the aggregated load response during DR control.  
 297 Zhang et al., 2013 introduced another state vector for the locked population, thus increasing  
 298 the complexity of the algorithm. However, it is difficult to obtain the real-time status of all  
 299 HVAC loads because of communication latency.

300

#### 301 4. Temperature Distribution Model for Aggregate HVAC Units

302 The basic principle of aggregate system analysis is to study the time-course evolution of  
 303 population instead of characterizing all individual HVAC units. Modeling and controlling of a  
 304 large population of HVAC units is a challenging task for at least two reasons. First, it takes a  
 305 long time, from minutes to hours, for the aggregated system to reach a stable state, but the  
 306 outdoor temperature keeps changing, pushing the control center to send out control  
 307 commands from time to time. The commands toggle some units' working state immediately.  
 308 The aggregated system runs under an unstable state most of the time. Second, most of the  
 309 control algorithms tend to change the HVAC unit's on/off state from time to time to result in  
 310 reduction of the unit's lifetime and fluctuations of overall power consumption. Zheng and  
 311 Cai (2014) evaluated this impact and found that the number of on/off cycles increased from  
 312 approximately 0–3 times per hour at normal to approximately 5–20 times per hour under DR  
 313 control. All these significantly increase the operating cost.

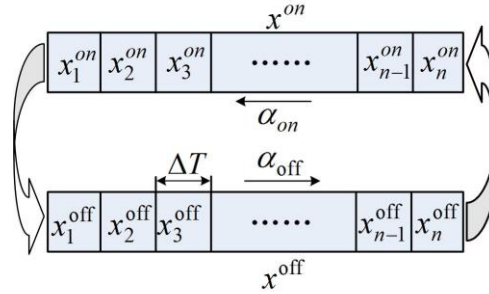
314

##### 315 4.1 Temperature Distribution Based on State-space

316 Based on the physical model of individual load discussed in Section 3, this section first  
 317 discusses the temperature distribution of HVAC loads for a large population (subsection 4.1).  
 318 Based on the distribution model, we analyzed the aggregated dynamics when adjusting the  
 319 population's setpoints (subsection 4.2) and the aggregated impact to the power system  
 320 (subsection 4.3).

321 Let  $[T_{a,\min}, T_{a,\max}]$  denote the inner air temperature range at a certain thermostat  
 322 setpoint. One can discretize this temperature range evenly into  $n$  small segments of

323 uniform width, resulting in a  $2n$  state-space model in Figure 2. At each segment, the unit  
 324 takes some time from entering to leaving; the difference in time at different temperature  
 325 segments shows the characteristics of the dynamic process.



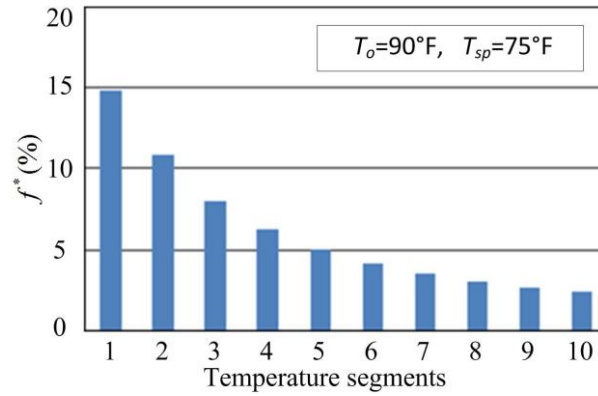
326  
 327 Figure 2 HVAC unit state-space transition model  
 328

329 The probabilities for an HVAC unit to reside in each of the  $2n$  states form the basis to  
 330 study the distribution of the aggregated loads. When an HVAC unit runs at a steady state  
 331 scenario, the inner air temperature evolves across the states. Temperature distribution  
 332 statistics were analyzed based on the simulation tests. A total of 2000 sets of physical  
 333 parameters are generated, which are randomly distributed around their nominal values with  
 334 a certain amount of variance, as described in Table 1. Each of them represents the real  
 335 condition in one house.

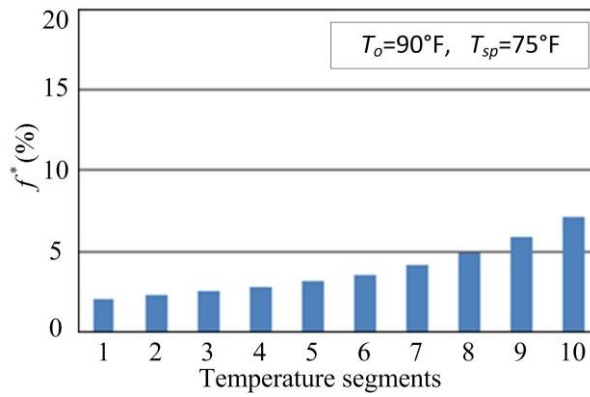
336 In this simulation test, this study sets the outdoor temperature  $T_o = 90$  °F, which remained  
 337 unchanged, and set all the units' cooling setpoint at  $T_{sp} = 75$ °F. When the population runs for  
 338 enough time, the aggregated system reaches a steady state, and the power consumption  
 339 becomes relatively stable. This study discredited the deadband into 10 segments uniformly  
 340 and obtained 20 different states to study the temperature distribution within the  
 341 temperature deadband. At any time, some of the loads reside in the ON states, moving  
 342 toward the lower limit of the temperature, while some others reside in the OFF states,  
 343 moving toward the upper limit. The objective of this subsection is to statistically analyze the  
 344 number of units in each state and calculate the proportion of them in all units. The  
 345 proportion of the units in segment  $i$  is calculated as follows.  
 346

347 
$$f_i^* = \frac{\Delta m_i^{on/off}}{n} \quad (2)$$

348 where  $\Delta m_i^{on/off}$  is the number of units of state on/off residing in the segment  $i$  at a  
 349 given moment and  $n$  is the total number of HVAC units, which is 2000 in this test case.  
 350 Figure 3 shows the units' temperature distribution over the states. It shows that the loads  
 351 are not uniformly distributed. For the "on" group, it becomes more dense as the  
 352 temperature reduces that means the speed of temperature evolution reduces near the  
 353 lower limit, as shown in Figure 3 a). It is the reverse distribution for the "off" group, as  
 354 presented in Figure 3 b).



a) Probability distribution of "ON" states



b) Probability distribution of "OFF" states

Figure 3 Probability Distribution of HVAC Units over ON/OFF states

The number of units staying in a specific state is estimated. The total power consumption is estimated by adding the number of units in all "on" states. We assume that all the units' power  $P$  and energy efficiency  $\eta$  are equal when their state is "on". The total power demand is then determined by the number of units in the "on" state at any time.

$$P_{HVAC}(t) = \frac{P}{\eta} \sum_{i=1}^n \Delta m_i \quad (3)$$

#### 4.2 System Evolution in Response to Control Commands

This study analyzed the dynamic process when adjusting units' setpoints using the temperature distribution model described in Section 4.1 and assumed that all HVAC units are working under the cooling mode. The basic principle of controlling the aggregate system is to adjust the population's thermostat setpoint, thus regulating the overall power consumption. The first case begins from the steady state described in subsection 4.1; the central controller sends a control command to raise the population thermostat setpoint by 0.4 °F; all HVAC units respond to control commands immediately. We redefine the states in the same pattern centered by the new setpoint, and then there are some "out-of-regime" states.

Figure 4 showed the system states in the temperature distribution model. The white block implies "out-of-regime" states. For the "off" state, the temperature of the "out-of-regime" states is lower than the new low limit. Therefore, the HVAC units take more time to increase

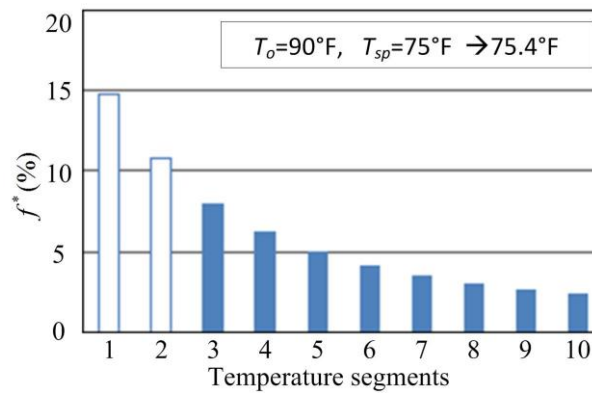
382 their temperatures to the new upper limit. However, for the “on” states, the HVAC units in  
 383 the “out-of-regime” states need to switch their state immediately. The instantaneous  
 384 increase in power of the entire system is expressed as follows.

$$385 \quad \Delta P = -\frac{P}{\eta} (m_1^{on} + m_2^{on}) \quad (4)$$

386  
 387 Figure 5 showed the instantaneous probability distribution when the central controller  
 388 sends out a command to decrease the population’s thermostat setpoint by 0.4 °F. For the  
 389 “on” states, the HVAC units of “out-of-regime” states need to work longer. The “off” states  
 390 need to switch “on” immediately. The amount of instantaneous power increased is  
 391 expressed as follows.

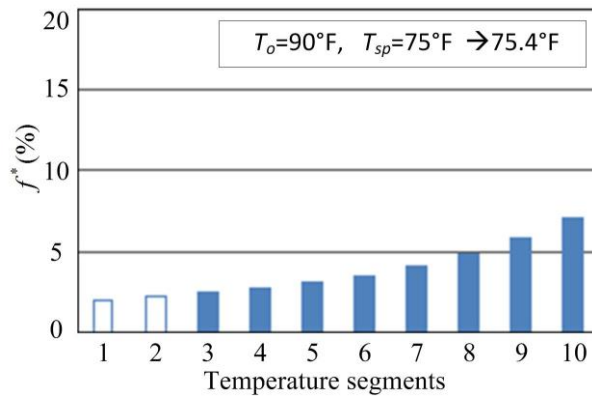
$$392 \quad \Delta P = \frac{P}{\eta} (\Delta m_9^{off} + \Delta m_{10}^{off}) \quad (5)$$

393



394  
 395  
 396

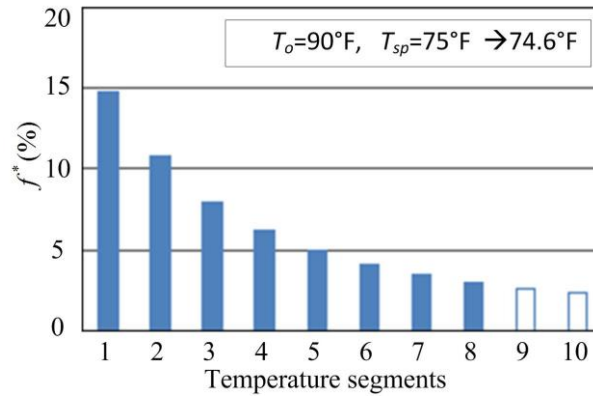
a) Instantaneous distribution of “ON” states



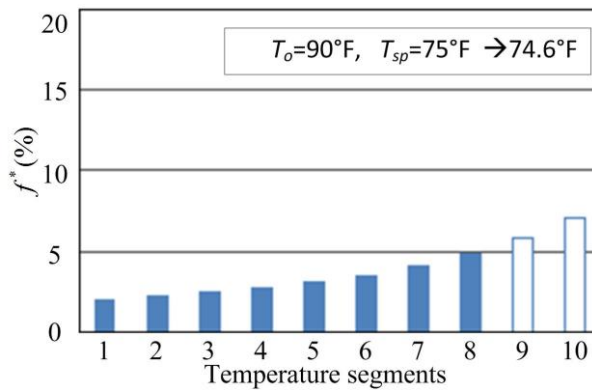
397  
 398  
 399  
 400  
 401  
 402

b) Instantaneous distribution of “OFF” states

Figure 4. Instantaneous probability distribution of the system after the thermostat setpoint is increased



a) Instantaneous distribution of "ON" states



b) Instantaneous distribution of "OFF" states

Figure 5. Instantaneous probability distribution of the system after decreases the thermostat setpoint

### 4.3 Power Fluctuation

The overall power consumption shows an immediate spike, followed by a damping oscillation process. A major contributor that affects the aggregate transient process is the diversity of the parameters of HVAC units. The highly homogeneous load populations often arouse strong oscillations, whereas a well-diversified load population undergoes a damping process with quick attenuation. In the literature, these observations are made mostly based on first-order thermostatically controlled load models; the second order ETP model of HVAC units also yields a similar behavior.

The oscillation process is validated against realistic simulations using GridLAB-D with thermostat setback programs, under different homogeneity of aggregate populations. In these two test cases, all the HVAC units participate in the same setback program where the set points are simultaneously shifted up from 75 °F to 76 °F at  $t=1$ (h) and released at  $t=4$ (h). The homogeneity of the population is controlled by reducing the parameters' distribution interval around their nominal values. The default distribution intervals are described in Table 1 (Adopted from Zhang et al. 2013). The quantified homogeneity of  $0.2 \delta_m$  is shown in Table 2. Detailed information about these parameters is provided in (GridLAB-D 2012).

Table 1. Default parameter values/distribution of the building used in GridLAB-D simulations (Adopted from Zhang et al. 2013)

Distribution	Value	Value
$U_c(\mu_{Af}, \delta_{Af})$ Uniform distribution of floor area	$U_c(2250,1500)$	Uniform(1500,3000)
$U_c(\mu_{Ia}, \delta_{Ia})$ Uniform distribution of air exchange	$U_c(0.625,0.75)$	Uniform(0.25,1)
$U_c(\mu_{Rc}, \delta_{Rc})$ Uniform distribution of roof R-value	$U_c(30,20)$	Uniform(20, 40)
$U_c(\mu_{Rw}, \delta_{Rw})$ Uniform distribution of wall R-value	$U_c(20,20)$	Uniform(10,30)
$U_c(\mu_{Rf}, \delta_{Rf})$ Uniform distribution of floor R-value	$U_c(22.5,25)$	Uniform(10,35)
$U_c(\mu_{Rd}, \delta_{Rd})$ Uniform distribution of door R-value	$U_c(3,4)$	Uniform(1,5)

432

433 Table 2. Parameters values/distribution of homogeneity  $0.2 \delta_m$

Distribution	Value	Value
$U_c(\mu_{Af}, 0.2\delta_{Af})$ Uniform distribution of floor area	$U_c(2250,300)$	Uniform(2100,2400)
$U_c(\mu_{Ia}, 0.2\delta_{Ia})$ Uniform distribution of air exchange	$U_c(0.625,0.15)$	Uniform(0.55,0.7)
$U_c(\mu_{Rc}, 0.2\delta_{Rc})$ Uniform distribution of roof R-value	$U_c(30,4)$	Uniform(28, 32)
$U_c(\mu_{Rw}, 0.2\delta_{Rw})$ Uniform distribution of wall R-value	$U_c(20,4)$	Uniform(18,22)
$U_c(\mu_{Rf}, 0.2\delta_{Rf})$ Uniform distribution of floor R-value	$U_c(22.5,5)$	Uniform(20,25)
$U_c(\mu_{Rd}, 0.2\delta_{Rd})$ Uniform distribution of door R-value	$U_c(3,0.8)$	Uniform(2.6,3.4)

434

435 Here,  $U_c(\mu_*, \delta_*)$  represents the uniform distribution centered by  $\mu_*$  and spans the  
436 distance  $\delta_*$ . For a uniform distribution in the range  $[V_*^-, V_*^+]$ :

$$437 \quad \mu_* = (V_*^- + V_*^+) / 2 \quad (6)$$

$$\delta_* = V_*^+ - V_*^-$$

438 To simplify the notation, we collect the parameters' distribution distance to form a  
439 parameter deadband vector as follows.

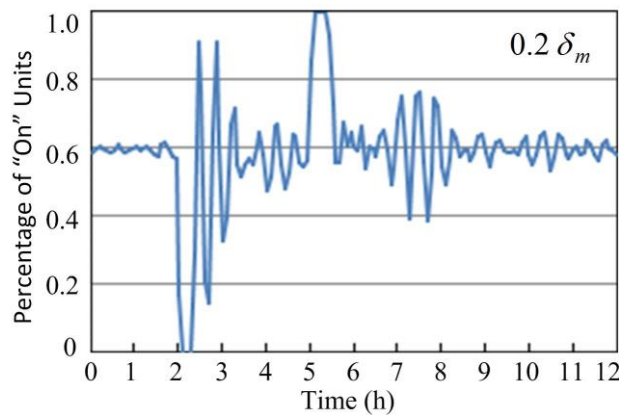
$$440 \quad \delta_m = [\delta_{Af}, \delta_{Ia}, \delta_{Rc}, \delta_{Rw}, \delta_{Rv}, \delta_{Rd}]^T \quad (7)$$

441 For the uniformly distributed parameters, keeping their center values unchanged, the load  
442 homogeneity is controlled by adjusting the parameters' distribution interval.

443

444 Figure 6-a) shows the percentage of "On" units of the population whose parameter  
445 distribution interval is  $0.2 \delta_m$ . In another simulation test, the parameter distribution intervals  
446 are decreased to  $0.1 \delta_m$ . The percentage of "On" units is shown in Figure 6 b).

447

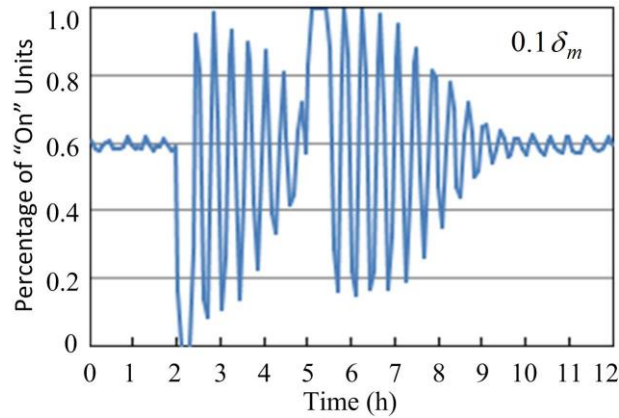


a) Parameter distribution interval is  $0.2 \delta_m$

448

449

450



b) Parameter distribution interval is  $0.1\delta_m$

451  
452  
453

Figure 6. Aggregated response of 1F setback program of different population homogeneities

455

### 5. Improved LSS Model

456

This study aims to improve the LSS mode as a new control method (Li et al. 2017). The key idea to maintain stability of power consumption is to preserve the diversity of temperature distribution of the aggregate population. This involves changing the way that HVAC loads respond to control commands. In practice, the LSS control mode can not eliminate load oscillations completely after a control action to preserve the diversity in the temperature distribution and reach a new steady state quickly instead of oscillating. Another distinguishing characteristic is that the LSS mode reduces the frequency of the HVAC unit's on/off switching.

464

#### 5.1 Designing of HVAC Units for Improved LSS Control

465

The units are not distributed uniformly among different temperature segments. There are more units in the segments near the limit where their working states are changed. This means that a small adjustment of the setpoint will cause many units to change their working states and cause serious power fluctuations.

466

The LSS method does not require any units to toggle any HVAC unit's working state immediately and tends to extend the units' working state as long as possible. Units of different working states act differently when the control center broadcasts a command to adjust the populations' thermostat setpoint. For example, when it needs to adjust load setpoint to a lower value, all "ON" state HVAC units execute the command immediately and maintain their "ON" state until the new lower limit  $T_-^{new}$ ; but all the "OFF" units do not execute the command. They just keep the command till the temperature reaches the upper limit  $T_+^{old}$ , and they execute the command to change their setpoint only after they change their working state to "ON". The flowchart of the DR system with the LSS is shown in Figure 7.

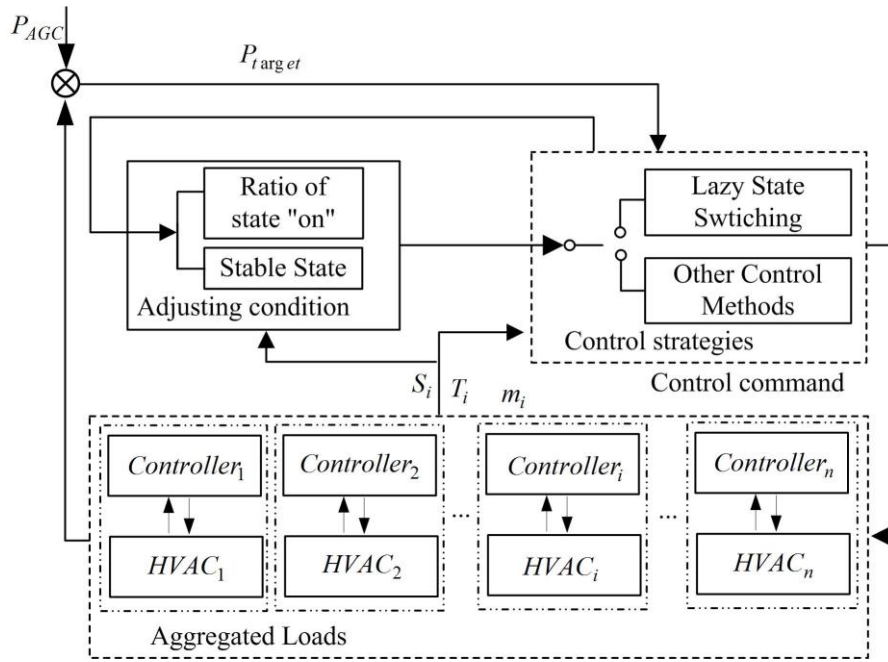
477

478

479

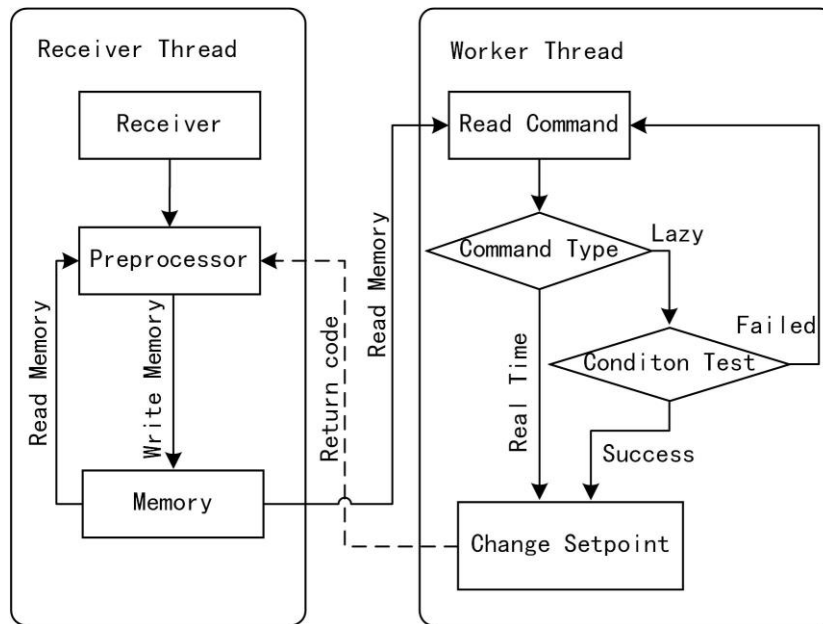
480

481



482  
483  
484  
485

a) Flowchart of DR system



486  
487  
488  
489

b) Flowchart of smart controller

Figure 7. Flowchart of DR system with LSS control

491  
492  
493  
494  
495  
496  
497

Figure 7 a) shows the structure of the control center that uses the ratio of “on” units ( $R_{on}$ ) and system stability condition as the switching indices to select the control strategy.  $R_{on}$  indicates the potential of system regulation. In the limit cases, if all units are “on”,  $R_{on}$  is 1, which means the aggregated loads cannot increase system power anymore; if all units are “off”,  $R_{on}$  is 0, which means there is no more power consumption to reduce. In contrast to other control methods, the LSS control requires each HVAC unit to be equipped with a smart

498 controller embedded in the HVAC unit or HEMS. Figure 7 b) indicates the logic process of the  
 499 smart controller handling the control command, which contains two working threads.

500 When a command is received, the receiver thread pass it to the preprocessor. The  
 501 preprocessor reads the shared memory, searches whether there exists a saved command,  
 502 and merges them together. For example, if there exists a command to increase the setpoint  
 503 by 1 °F, and the new command is to decrease the setpoint by 0.4 °F; then the merged  
 504 command is to increase the setpoint by 0.6 °F. Then, the preprocessor saves the merged  
 505 command to the memory.

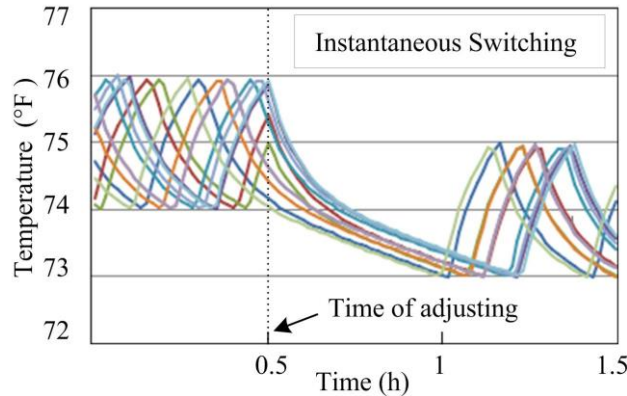
506 The worker thread reads the shared memory periodically to check the command type and  
 507 executes it in different ways according to the command type. If the command is a lazy one,  
 508 the thread will do a condition test. The worker thread executes the command after the  
 509 conditions are met. It then transfers the return code to the preprocessor to handle the saved  
 510 command. The command cannot be executed until the condition is satisfied. The HVAC unit  
 511 condition switch is expressed as follows.

$$512 \quad T_{sp,i}(t) = \begin{cases} T_{sp,i}(t - \varepsilon_t) & S(t - \varepsilon_t) = 0 \\ & \& \Delta T_{sp}(t - \varepsilon_t) \cdot [T_{sp,i}(t - \varepsilon_t) - T_o] < 0 \\ T_{sp,i}(t - \varepsilon_t) + \Delta T_{sp}(t - \varepsilon_t) & S(t - \varepsilon_t) = 1 \\ & \& \Delta T_{sp}(t - \varepsilon_t) \cdot [T_{sp,i}(t - \varepsilon_t) - T_o] > 0 \end{cases} \quad (8)$$

513

## 514 5.2 Improved Response Mode of Individual HVAC units

515 This study begins from the steady state with  $U_{set} = 75^\circ\text{F}$ ,  $\delta = 2^\circ\text{F}$ ,  $T_o = 90^\circ\text{F}$  to examine  
 516 the effects of the individual and aggregate dynamics of HVAC under LSS control mode when  
 517 adjusting the setpoint. The setpoint is reduced by 1 °F. Figure 8 a) shows the inner air  
 518 temperature trajectories of ten samples with instantaneous switching in other control  
 519 modes. Figure 8 b) shows air temperature trajectories under the LSS mode of ten samples.  
 520

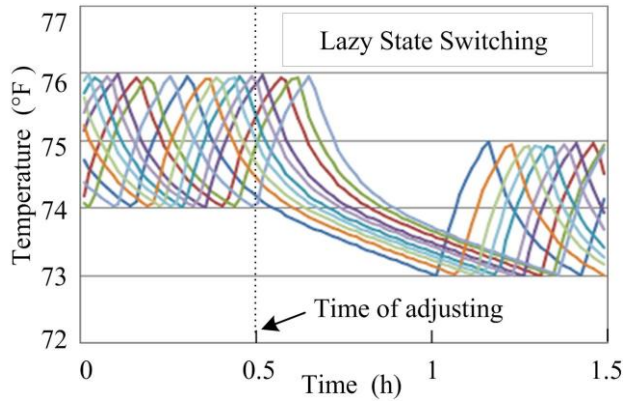


521

522

523

a) Ten samples with instantaneous switching



b) Ten samples with LSS control

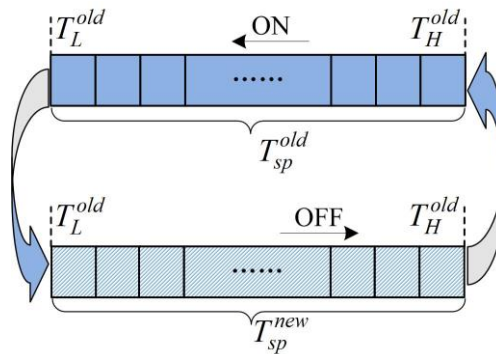
Figure 8. Temperature trajectories of ten samples

In the case of instantaneous switching, all the loads adjust their on/off states according to the new setpoint immediately after receiving the control command. There is a serious impact on the diversity of the aggregated loads after the control actions. However, under LSS control, some loads satisfying the switching condition execute the command and keep working till the new temperature limit is reached; others keep their working state until they reach the older temperature limits.

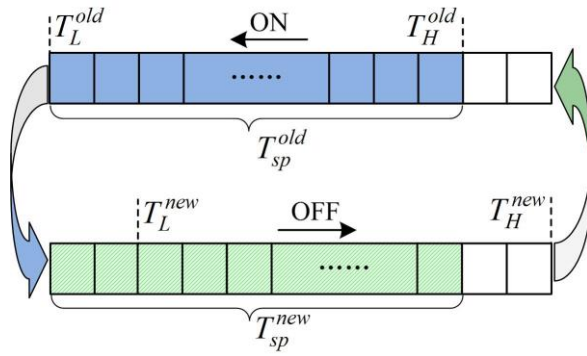
### 5.3 Preservation of Diversity in HVAC unit Air Temperature

This subsection discusses the load temperature distribution dynamics when adjusting the system thermostat setpoint. The key to maintain a stable power consumption is to maintain the diversity of the aggregate population of HVAC units. To illustrate the improvement of LSS control mode, we examine the load diversity changes when adjusting the system setpoint.

Previous studies have attempted to improve the aggregate control. Their main drawback is that they tried to control all units instantly and tried to avoid the lockout constraints based on a large operational cost. Figure 9 shows the system state evolution process when the system is controlled to increase the setpoint under the LSS control mode.

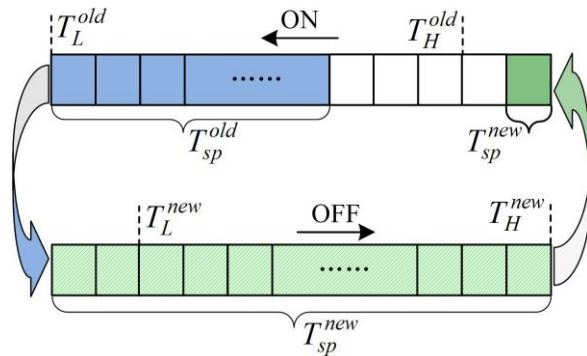


a) Temperature distribution under the initial setpoint



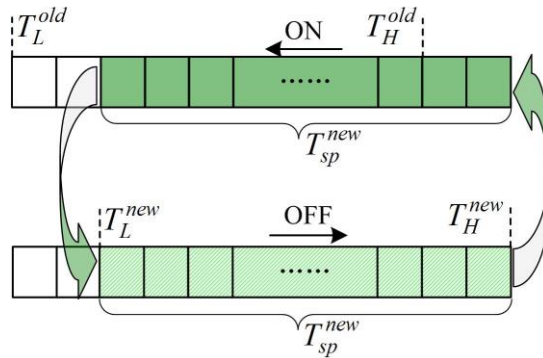
550  
551  
552

b) Temperature distribution after receiving the adjusting command



553  
554  
555

c) Temperature distribution in the middle of the transition process



556  
557  
558

d) Temperature distribution at the end of the transition process

Figure 9. Density evolution of the process when shifting up the population's setpoint

560

## 6. Discussions

562

Two high homogeneity scenarios are studied to evaluate the proposed control method to illustrate the adaptability and performance of the proposed control method. The stability of the aggregated loads is illustrated by varying the percentage of "ON" units. The proposed aggregate model provides a robust control mechanism for large populations of HVAC units. We use the same setback program that shifts the population's thermostat setpoint by 1 °F higher at  $t = 2$  h and changes it back at  $t = 5$  h. Figure 10 shows the dynamic process of 2000 HVAC units of different homogeneities.

569

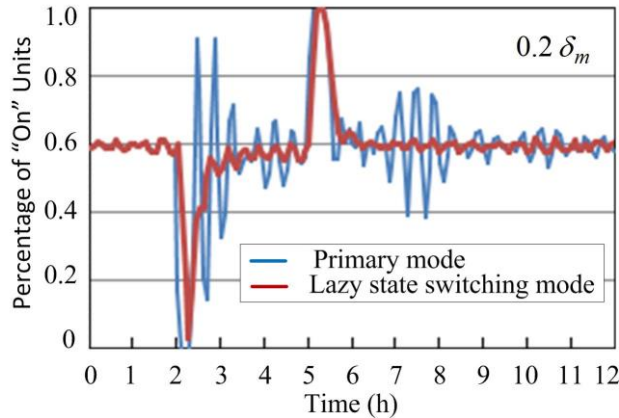
Under the LSS control mode, the aggregate HVAC system's response curve follows the red line in Figure 10. This study notes the following observations:

570

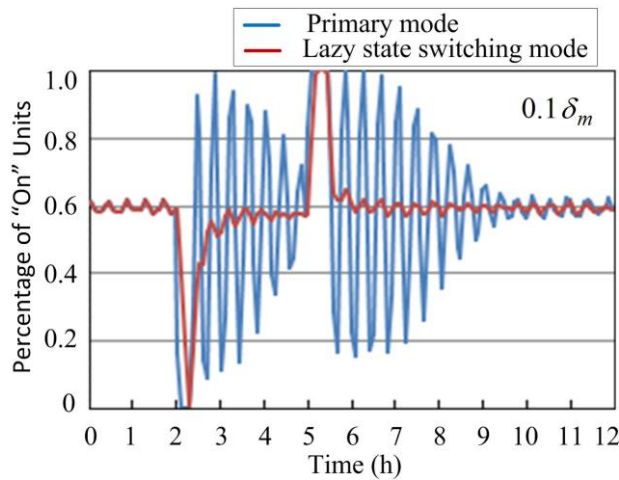
1. The initial spike is weaker and a little late, which comes with a climbing process. The

571

- 572 power flickers and fluctuations disappeared, which is inevitable under instantaneous  
 573 switching control methods.
- 574 2. There was almost no succeeding fluctuation under the proposed control mode.
  - 575 3. The proposed model tends to maintain the working states of the HVAC units and  
 576 protects the unit from overuse.
  - 577 4. The frequency of HVAC units' on/off switching would be lower than normal operation  
 578 because HVAC units are controlled to prolong their work cycle from time to time.  
 579  
 580



581 a) Unit parameter distribution interval is  $0.2 \delta_m$  of the default intervals  
 582  
 583



584 b) Unit parameter distribution interval is  $0.1 \delta_m$  of the default intervals  
 585

586 Figure 10. Aggregate responses under setback program with different parameter distribution  
 587 intervals  
 588

589 The stability of the aggregated system can not only improve power quality but also  
 590 improve the ability to respond to signals. The aggregated loads cannot track AGC signals  
 591 until the system achieves a stable condition. A good performance in the stability of power  
 592 consumption shows the potential of the proposed model to improve power quality in the  
 593 control of aggregate HVAC systems.

594 However, this study is subject to a number of uncertainties. (1) The weather conditions  
 595 are associated with considerable uncertainties. Various parameters and evolution speeds  
 596 have a direct impact on HVAC units in a complicated way. The time scale beneath which  
 597 HVAC systems work are comparable significantly to weather conditions; therefore, to control

598 and adjust the aggregate system, this study considers the trends of weather variations; and  
599 (2) the first spike with a large amplitude and long duration time still exists, and other  
600 resources are required to balance the power variation. The amplitude and interval of system  
601 regulation are limited by the compensation capability of other resources. Third, there are  
602 unavoidable uncertainties including users' preferences and unexpected operations.

603

## 604 **7. Conclusion**

605 This study improved the LSS control mode to provide secondary frequency regulation  
606 in a fully developed smart grid environment, which fully adapted to the slow response and  
607 operation constraints of HVAC systems. The LSS mode shows promising performance in  
608 maintaining the diversity of inner air temperature distribution of units in the aggregate  
609 system. It is essential for an aggregated system to restore stability after control actions and  
610 get ready quickly to track the next AGC signals. Traditional control methods tend to monitor  
611 the system status in real time, which is always accompanied by a high operation cost.

612 In contrast to traditional control methods, the LSS control mode has a minor requirement  
613 for real-time monitoring of HVAC' working states and does not require any unit to interrupt  
614 its working state. This study tends to extend some units' work cycles, which preserves the  
615 population's state diversity during the adjustment. For individual HVAC units, the LSS mode  
616 can reduce the frequency of the unit's on/off switching, which protects them from overuse.  
617 The power consumption is quickly restored to a stable state, thus making it easy for the  
618 utilities to improve DR applications based on HVAC systems. Integrated with other resources,  
619 the aggregate HVAC system adjusts the overall power consumption within limits and  
620 improves the efficiency and controllability of the whole system.

621 Future study is required to adapt the proposed control method to a changing ambient  
622 temperature and to develop adaptive control algorithms for the control center. Others  
623 should focus on integrating the LSS mode with other control algorithms to achieve better  
624 results. This study may provide valuable and useful ideas for researchers and industrialists  
625 working to develop better control methods. It is hoped that these novel methods will help  
626 improve the renewable usage and power quality in future smart grids.

627

## 628 **ACKNOWLEDGMENT**

629 This work was supported by the Natural Science Foundation of Hebei Province (No.  
630 E2018202282) and Natural Science Foundation of Tanjin Key Project (No. 19JCZDJC32100).

631

## 632 **REFERENCES**

- 633 1. Abdul, M.H., Naomitsu U., Ahmed, Y.S., 2014. Control Strategies for Wind Farms Based  
634 Smart Grid System, *IEEE Trans. on Industry Applications* 50, 3591-3601.
- 635 2. Adhikari, R., Pipattanasomporn, M., Rahman, S., 2018. An algorithm for optimal  
636 management of aggregated HVAC power demand using smart thermostats. *Applied*  
637 *Energy* 217, 166-177.
- 638 3. Antti, P., Madis, T., Klaus, C., Jan, H.1, 2019. Designing an organizational system for  
639 economically sustainable demand-side management in district heating and cooling.  
640 *Journal of Cleaner Production* 219. 433-442.
- 641 4. Bashash, S., Fathy, H.K., 2013. Modeling and Control of Aggregate Air Conditioning Loads  
642 for Robust Renewable Power Management. *IEEE Trans. Control Systems Technology* 21,  
643 1318-1327.

- 644 5. Beil, I., Hiskens, I., Backhaus, S., 2016. Frequency regulation from commercial building  
645 HVAC demand response. *Proceedings of the IEEE* 104, 745 – 757.
- 646 6. Bidram, A., Davoudi, A., 2012. Hierarchical Structure of Microgrids Control System. *IEEE*  
647 *Trans. Smart Grid* 3, 1963-1976
- 648 7. Cai, J., Braun, J.E., 2019. A regulation capacity reset strategy for HVAC frequency  
649 regulation control. *Energy and Buildings* 185, 272-286.
- 650 8. Cui, H.B., Zhou, K.L., 2018. Industrial power load scheduling considering demand  
651 response. *Journal of Cleaner Production* 204, 447-460.
- 652 9. Eksin, C., Deliç, H., Ribeiro, A., 2015. Demand Response Management in Smart Grids With  
653 Heterogeneous Consumer Preferences. *IEEE Trans. Smart Grid* 6, 3082-3094.
- 654 10. Ghanem, D. A., Mander, S., 2014. Designing consumer engagement with the smart grids  
655 of the future: bringing active demand technology to everyday life. *Technology Analysis &*  
656 *Strategic Management* 26, 1163–1175.
- 657 11. GridLAB-D Simulation Software Documentation (2012) GridLAB-D Residential Module  
658 User’s Guide. SourceForge official website. Available:  
659 [http://gridlab-d.sourceforge.net/wiki/index.php/Residential\\_module\\_user%27s\\_guide](http://gridlab-d.sourceforge.net/wiki/index.php/Residential_module_user%27s_guide).
- 660 12. Giwa, S. O., Nwaokocha, C. N., & Adeyemi, H. O. (2019). Noise and emission  
661 characterization of off-grid diesel-powered generators in Nigeria. *Management of*  
662 *Environmental Quality: An International Journal*, 30(4), 783-802.
- 663 13. Hamidreza. J., Hanif, T., Ali, A., Masoud, A.G., Jaume, M., Mohammad, T., Gao, H.O.,  
664 2019. Charging demand of Plug-in Electric Vehicles: Forecasting travel behavior based on  
665 a novel Rough Artificial Neural Network approach. *Journal of Cleaner Production* 229,  
666 1029-1044.
- 667 14. Hao, H., Sanandaji, B.M., Poolla, K., Vincent, T.L., 2015. Aggregate Flexibility of  
668 Thermostatically Controlled Loads. *IEEE Trans. Power System* 30, 189–198.
- 669 15. Ismail, T.M., Ramzy, K, Elnaghi, B.E., Abelwhab, M.N., El-Salam, M.A., 2019. Using  
670 MATLAB to model and simulate a photovoltaic system to produce hydrogen. *Energy*  
671 *Conversion and Management* 185, 101-129.
- 672 16. Ji, H.Y., Ross, B., Atila, N., 2014. Dynamic Demand Response Controller Based on  
673 Real-Time Retail Price for Residential Buildings. *IEEE Trans. Smart Grid* 5, 121-129.
- 674 17. Jin, M., Feng, W., Marnay, C., Spanos, C., 2018. Microgrid to enable optimal distributed  
675 energy retail and end-user demand response. *Applied Energy* 210, 1321-1335.
- 676 18. Jordehi, A.R., 2019. Optimisation of demand response in electric power systems, a  
677 review. *Renewable and Sustainable Energy Reviews* 103, 308-319.
- 678 19. Kabache, N., Moulahoum, S., Houassine, H., 2014. Experimental Investigation of  
679 Self-excited Induction Generator for Insulated Wind Turbine. *Journal of Electrical*  
680 *Engineering* 14. 1-10.
- 681 20. Khasawneh, H. J., Illindala, M. S., 2014. Battery cycle life balancing in a microgrid through  
682 flexible distribution of energy and storage resources. *Journal of Power Sources* 261,  
683 378-388.
- 684 21. Li, L.L., Chen, X.D., Tseng, M.L., Wang, C.H., Wu K.J., Lim, M.K., 2017. Effective power  
685 management modeling of aggregated heating, ventilation, and air conditioning loads  
686 with lazy state switching. *Journal of Cleaner Production* 166, 844-850.
- 687 22. Lu, N., 2012. An Evaluation of the HVAC Load Potential for Providing Load Balancing  
688 Service. *IEEE Trans. Smart Grid* 3, 1263-1270.
- 689 23. Lu, N., Chassin, D.P., 2004. A state-queueing model of thermostatically controlled  
690 appliances. *IEEE Trans. Power Systems* 19, 1666-1673.

- 691 24. Lu, N., Chassin, D.P., Widergren, S.E., 2005. Modeling Uncertainties in Aggregated  
692 Thermostatically Controlled Loads Using a State Queueing Model. *IEEE Trrans. Power*  
693 *System* 20, 725-733.
- 694 25. Ma, K., Yuan, C.L., Yang, J., Liu, Z.X., Guan, X.P., 2017. Switched Control Strategies of  
695 Aggregated Commercial HVAC Systems for Demand Response in Smart Grids. *Energies* 10,  
696 doi:10.3390/en10070953.
- 697 26. Ma, Z., Ren, H., Lin, W., 2019. A review of Heating, Ventilation and Air Conditioning  
698 technologies and innovations used in solar-powered net zero energy Solar Decathlon  
699 houses. *Journal of Cleaner Production*, <https://doi.org/10.1016/j.jclepro.2019.118158>
- 700 27. Malik, A., Ravishankar, J., 2018. A hybrid control approach for regulating frequency  
701 through demand response. *Applied Energy* 210, 1347-1362.
- 702 28. Muhammad, A.S.H., Chen, M.Y., Lin, H.L., Mohammed, H.A., Muhammad, Z.K., Gohar,  
703 R.C., 2019. Optimization modeling for dynamic price based demand response in  
704 microgrids. *Journal of Cleaner Production* 222, 231-241.
- 705 29. Müller, F.L., Jansen, B., 2019. Large-scale demonstration of precise demand response  
706 provided by residential heat pumps. *Applied Energy* 239, 836-845.
- 707 30. Nguyen, D.T., Le, L.B., 2014. Joint optimization of electric vehicle and home energy  
708 scheduling considering user comfort preference. *IEEE Trans. Smart Grid* 5, 188–199.
- 709 31. Parrish, B., P., Gross, R., Heptonstall, P., 2019. On demand: Can demand response live up  
710 to expectations in managing electricity systems?. *Energy Research & Social Science*  
711 Volume 51, 107–118.
- 712 32. Pourmousavi, S. A., Patrick, S. N., Nehrir, M. H., 2014. Real-Time Demand Response  
713 Through Aggregate Electric Water Heaters for Load Shifting and Balancing Wind  
714 Generation. *IEEE Trans. Smart Grid* 5, 769-778.
- 715 33. Sedady, F., & Beheshtinia, M. A. (2019). A novel MCDM model for prioritizing the  
716 renewable power plants' construction. *Management of Environmental Quality: An*  
717 *International Journal*, 30(2), 383-399.
- 718 34. Tindemans, S.H., Trovato, V., Strbac, G., 2015. Decentralized Control of Thermostatic  
719 Loads for Flexible Demand Response. *IEEE Trans. Control Syst.Technol.* 23, 1685–1700.
- 720 35. Wang, D., Ge, S.Y., Jia, H.J., Wang, C.S., Zhou, Y., Lu, N., Kong, X.Y., 2014. A demand  
721 response and battery storage coordination algorithm for providing microgrid tie-line  
722 smoothing services. *IEEE Trans. Sustainable Energy* 5, 476-486.
- 723 36. Wei, T., Zhu, Q., Yu, N., 2016. Proactive Demand Participation of Smart Buildings in Smart  
724 Grid. *IEEE Transactions on Computers* 65, 1392-1406.
- 725 37. Vakiloroaya, V., Samali, B., Fakhar, A., Pishghadam, K., 2014. A review of different  
726 strategies for HVAC energy saving. *Energy Conversion and Management* 77, 738-754.
- 727 38. Vanouni, M., Lu, N., 2015. Improving the Centralized Control of Thermostatically  
728 Controlled Appliances by Obtaining the Right Information. *IEEE Trans. Smart Grid* 6,  
729 946-948.
- 730 39. Yan, S., Tan, S., Lee, C., Chaudhuri, B., Hui, S.Y.R., 2017. Use of Smart Loads for Power  
731 Quality Improvement. *IEEE Journal of Emerging and Selected Topics in Power Electronics*  
732 5, 504-512.
- 733 40. Yin, R.G., Emre, C.K., Li, Y.Pl., Nicholas, D., Wang, K., Yong, T.Y., Michael, S., 2016.  
734 Quantifying flexibility of commercial and residential loads for demand response using  
735 setpoint changes. *Applied Energy* 177, 149–164.
- 736 41. Zhang, W., Lian, J.M., Chang, C.Y. Kalsi, K., 2013. Aggregated Modeling and Control of Air  
737 Conditioning Loads for Demand Response. *IEEE Trans. Power Systems* 28, 4655-4664.

738 42. Zheng, L., Cai, L., 2014. A Distributed Demand Response Control Strategy Using Lyapunov  
739 Optimization. IEEE Trans. Smart Grid 5, 2075-2083.

740 43. Zhou, Y., Wang, C., Wu, J., W, J., C.M., Li, G., 2017. Optimal Scheduling of Aggregated  
741 Thermostatically Controlled Loads with Renewable Generation in the Intraday Electricity  
742 Market. Applied Energy 188, 456–465.

743 44. Zhu, L., Yan, Z., Lee, W.J., Yang, X., Fu, Y., Cao, W., 2015. Direct Load Control in  
744 Microgrids to Enhance the Performance of Integrated Resources Planning. IEEE Trans.  
745 Industry Applications 51, 3553-3560.

746

747

748